

High-precision wavelength-flexible frequency division for metrology

Petra Groß* and Klaus-Jochen Boller

Department of Applied Physics, University of Twente, 7500 AE Enschede, The Netherlands

Marvin E. Klein

Art Innovation b.v., Zutphenstraat 25, 7575 EJ Oldenzaal, The Netherlands

(Received 14 December 2004; published 29 April 2005)

We realize and investigate wavelength-flexible phase-coherent all-optical frequency division by 2. Frequency division is obtained via self-phase-locking in a degenerate continuous-wave (cw) optical parametric oscillator (OPO). The wavelength flexibility of the divider is based on the use of quasi-phase-matching with perpendicular polarizations of the OPO output waves (type II). Mutual injection of the subharmonic waves is achieved by using an intracavity quarter-wave plate. A locking range of up to 160 MHz is observed experimentally, and a stable, self-phase-locked operation of the OPO is achieved over typically 15 min. For the first time, we measure the frequency stability of the divider by recording the relative phases of the subharmonic waves as a function of time. For a measurement time interval of 40 s, we measure a residual frequency instability of the divider of 8×10^{-18} . We demonstrate a full control of the OPO's output-wave phase difference and observe the related change in power ratio of the subharmonic waves in agreement with the theoretically expected behavior. We propose that this possibility to monitor the divider's drift within the locking range via the power ratio can be used for stabilizing that drift in order to achieve a significant improvement of the long-term stability of the divide-by-2 OPO.

DOI: 10.1103/PhysRevA.71.043824

PACS number(s): 42.62.Eh, 42.65.Yj, 42.65.Lm

I. INTRODUCTION

Due to their unique coherence properties, continuous-wave (cw) optical parametric oscillators (OPO's) operating at or close to frequency degeneracy are particularly well-suited candidates for applications in quantum optics. The intensity correlation of the two generated waves has been exploited for twin-beam generation [1,2], and their frequency correlation has found useful application in coherent control schemes [3]. The phase correlation of a phase-locked OPO offers a potentially high precision, which makes these optical frequency dividers powerful tools for frequency metrology [4]. OPO's offer indispensable properties like a high efficiency, which is a prerequisite for a high signal-to-noise ratio, together with a potential for a narrow linewidth. Furthermore, they can be designed (e.g., using quasi-phase-matching nonlinear crystals) such that they can be taken into operation over a wide spectral region.

It is well known that the sum of the phases of any OPO subharmonic waves follows the pump phase, while their difference phase undergoes a phase diffusion process [5]. In order to achieve phase-coherent frequency division, this diffusion process has to be counteracted, which can be achieved either via an electronic servoloop [6–8] or by an optical phase-locking process. As compared to an electronic control, an all-optically phase-locked frequency divider is expected to provide a higher precision due to a shorter response time.

To control the output phases of an OPO divider in an all-optical manner, one of the output waves can be phase locked by injecting another wave, similar to injection locking

of lasers [9]. If the injected wave is generated within the OPO itself, the method may be termed self-phase-locking. All-optical frequency division by 3 through self-phase-locking has been demonstrated in our previous work with a cw OPO [10]. The most straightforward approach for a self-phase-locked divide-by-2 OPO seems to be a frequency-degenerate, type-I phase-matched OPO, where the polarizations of the OPO subharmonic waves are parallel such that the signal wave locks the idler wave and vice versa. Such self-phase-locking has been observed qualitatively [11]; however, type-I phase-matched OPO's near degeneracy usually reveal an enormously wide gain bandwidth and other severe tuning difficulties that hamper spectral control [6]. Near frequency degeneracy, type-II phase-matched OPO's—i.e., with orthogonally polarized subharmonic waves—are better suited for precise frequency division, because the dispersion of the signal and idler wave in the crystal is different, which considerably narrows the gain bandwidth and thus allows for fine frequency tuning via the phase-matching parameters and good frequency stability. Self-phase-locking in such an OPO can be achieved by inserting a quarter-wave plate in the OPO cavity as was demonstrated first by Mason and Wong [12].

The approach taken in that previous work is, however, much limited with respect to the optical frequencies that can be divided, as a consequence of using noncritical phase matching in birefringent crystals. This restricts the applicability of such divide-by-2 OPO's in precision frequency metrology. In this paper, we present and characterize an alternative approach to all-optical frequency division by 2. Contrary to former work, this divider maintains full wavelength flexibility, which is demonstrated by dividing an arbitrary near-infrared frequency from a tunable diode laser. This flexibility is obtained by using quasi-phase-matching in an

*Electronic address: p.gross@utwente.nl

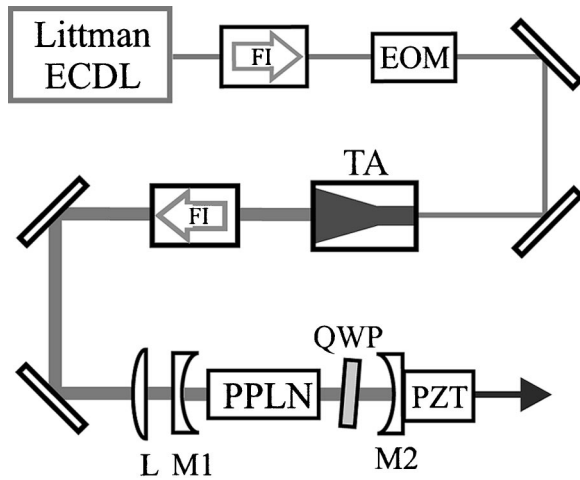


FIG. 1. Setup of the divide-by-2 OPO. Littman ECDL, Littman external cavity diode laser; FI, Faraday isolator; EOM, electro-optic modulator for electronic stabilization of the OPO cavity length; TA, tapered amplifier; L , lens; $M1$, $M2$, cavity mirrors; PPLN, periodically poled lithium niobate crystal; QWP, quarter-wave plate; PZT, piezo transducer.

unusual (type-II) polarization geometry. We measure the locking range as a function of the strength of mutual signal-idler injection, which can be continuously adjusted via the rotation of a cavity-internal quarter-wave plate, as in Ref. [12]. We present the first measurement of the subharmonic phase difference in a self-phase-locked OPO as a function of time, which allows for a determination of the divider's residual frequency instability. With this we observe the frequency instability of the divider to be as low as 8×10^{-18} for a measurement time interval of 40 s. Our monitoring of the phase difference and output power ratio of the subharmonic waves shows excellent agreement with the theory on self-phase-locked frequency division by 2. This proves that the divider's phase difference, which depends on the detuning of the cold cavity modes from the pump frequency exactly divided by 2 [13,14], can be easily monitored via the subharmonic power ratio.

II. EXPERIMENTAL SETUP AND CHARACTERISTICS OF THE OPO

A. Setup

The experimental setup of the OPO frequency divider is shown in Fig. 1. The frequency to be divided is provided by a single-frequency AlGaAs diode master-oscillator power-amplifier (MOPA) system with a wavelength tuning range of about 25 nm around 800 nm [15]. The master oscillator is a single-stripe diode laser in a Littman external grating cavity [16]. Via rotation of the feedback mirror, we have set the output wavelength to a value of 801.8 nm, at which a near diffraction-limited output beam with a maximum power of 360 mW is available behind the amplifier and a 60-dB optical isolator.

The triply resonant two-mirror OPO is similar to the one described in Ref. [12]. The OPO is based on quasi-phase-

matching (QPM) in a crystal of periodically poled lithium niobate (PPLN). Contrary to the common choice of type-I QPM (parallel polarizations for accessing the largest nonlinear coefficient of the crystal), we decided for type-II QPM with crossed polarizations of the signal and idler wave. This choice is expected to significantly narrow the spectral gain bandwidth and thus enable a spectrally stable operation of the OPO also near frequency degeneracy. For type-II QPM, the 50-mm-long PPLN crystal carries a poling period of 10.1 μm for frequency-degenerate operation of the OPO. In this case, one of the subharmonic waves is ordinary polarized (parallel to the pump wave), while the other subharmonic wave is extraordinary polarized; hence, throughout this paper we term the two subharmonic waves the e-wave and the o-wave. The crystal faces are intentionally wedged at about 0.72° with respect to each other, such that a transverse displacement of the crystal can be used to fine-tune the optical length of the crystal in the OPO cavity.

The crystal is placed at the center of a symmetric two-mirror linear cavity, where the two mirrors each have a radius of curvature of 50 mm and are separated by 120 mm, which provides a beam waist of $w_0=46 \mu\text{m}$ for the fundamental cavity mode of the pump wave. The pump input mirror $M1$ is highly reflective for the OPO subharmonic waves and has a transmission of 15% at the pump wavelength. The output coupling mirror $M2$ is highly reflective at the pump wavelength and provides output coupling of each of the subharmonic waves of 1%. For stable cw operation, the cavity length is stabilized to the pump wavelength with an electro-optic modulator (EOM) and a piezo transducer (PZT) behind $M2$ using the Pound-Drever-Hall technique [17].

A quarter-wave plate (QWP) in the OPO cavity serves for an adjustable amount of mutual injection of the two subharmonic waves. The QWP is antireflection coated for the pump and subharmonic wavelengths.

B. OPO output power

When the OPO is operated without the intracavity quarter-wave plate, the threshold pump power is approximately 140 mW and the output power is about 4 mW for each of the subharmonic waves at the maximum available pump power of 360 mW. Increasing the output coupling from 1% to 2% for the subharmonic waves, the OPO generates 16 mW of subharmonic power, but at the same time the threshold increases to 170 mW.

The OPO output power has been measured with the quarter-wave plate being inserted into the cavity and set to various rotation angles. The values obtained for the slope efficiency and the threshold pump power are used to determine the experimental cavity losses as described in Ref. [18]. From these measurements, we obtain about 6% single-pass losses for the e-wave and about 6.3% for the o-wave. The passive single-pass losses for the pump without the QWP are 8.7%, and inserting the QWP causes an increase of the pump losses to $10.1\% + 0.25\%$ per degree of the QWP rotation angle. With these passive losses and using a mirror with 1% output coupling for the subharmonic waves, the OPO can be operated with a QWP rotation angle of up to 6° at the given

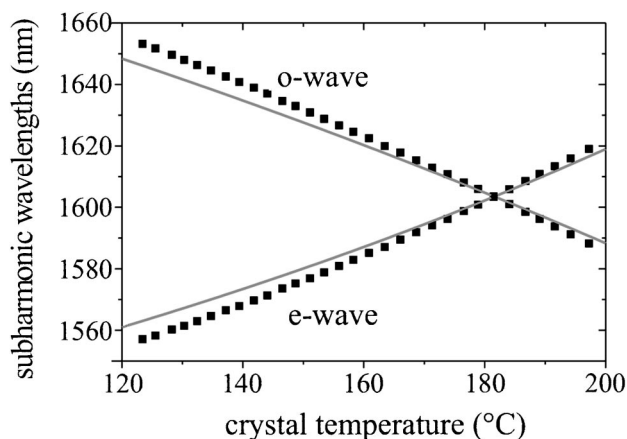


FIG. 2. Subharmonic wavelengths as a function of the crystal temperature. Symbols: measured values. Solid line: theoretical tuning derived from the Sellmeier coefficients given in Ref. [19].

maximum pump power. All of the experiments described below are carried out using this setup.

C. Wavelength tuning

The OPO output wavelengths were coarsely tuned by changing the crystal temperature. Figure 2 shows the wavelength tuning, measured with an optical spectrum analyzer (OSA). By changing the crystal temperature from 123 to 197 °C, the wavelength of the o-wave decreases from 1653 to 1590 nm, while the e-wavelength increases from 1557 to 1620 nm. At a temperature of 181.5 °C, the wavelength curves intersect at the doubled value of the pump wavelength—i.e., at 1603.6 nm.

With the described tuning and within the resolution capability of the OSA it is possible to bring the subharmonic waves as close to wavelength degeneracy as 0.05 nm, which corresponds to a frequency difference of the e- and o-waves of 6 GHz. This is, however, too coarse to reliably tune the OPO across its range of self-frequency-locking, which is expected to be on the order of 100 MHz. To enable a measurement of the frequency difference between the two subharmonic waves on a MHz scale, we observe their beat frequency. For this, the two subharmonic waves are projected onto a common polarization axis using a polarizer and then directed onto a fast photodiode, followed by an rf amplifier and an rf spectrum analyzer.

If the OPO subharmonic frequencies ν_e and ν_o are sufficiently close to each other such that their beat can be detected with the used setup (i.e., $\delta\nu = |\nu_e - \nu_o| < 2.5$ GHz as given by the cutoff frequency of the photodiode amplifier), the beat frequency is further tuned towards zero. This is achieved via combined changes of the crystal temperature and a lateral translation of the crystal. The latter results in a change of the crystal length, due to the wedged crystal faces. Each of the two tuning methods simultaneously changes the optical cavity lengths of the e-wave, the o-wave, and the pump wave, though with a different rate. We note that a change of the optical cavity length for the pump wave is fully compensated by a piezo translation of mirror $M2$ due to

the electronic Pound-Drever-Hall cavity stabilization. However, changes of the optical cavity lengths for the e- and o-waves are not fully compensated, such that these waves tune with respect to each other. In the case that the OPO is free running—i.e., not phase-locked—the resulting change of the e- and o-wave cavity modes is observable as a tuning of the e-o-beat frequency.

By applying only either one tuning method separately—i.e., by changing the crystal temperature or the crystal's lateral position—a rather limited range of continuous tuning of the beat frequency (up to 36 MHz) is achieved, which unavoidably is followed by a subharmonic mode hop seen as a jump of the beat signal by 1.7 GHz, corresponding to twice the free spectral range of the cavity. By combining the two tuning methods, however, their continuous tuning ranges can be iteratively overlapped, yielding a continuous tuning range of the beat frequency over more than 400 MHz. This is well sufficient to tune the OPO frequencies into and through the entire locking range, with any given starting constellation of cavity detunings.¹

III. EXPERIMENTAL RESULTS

A. Locking range

In order to measure the locking range, the beat frequency is tuned toward zero using the described iterative tuning. In the vicinity of zero beat frequency, the beat signal is expected to vanish when optical self-phase-locking occurs [20].

Figure 3 shows the measured beat signal power as a function of the beat frequency for the two cases that the quarter-wave plate rotation angle ϑ_{QWP} was set to 0° [Fig. 3(a)] and to 3° [Fig. 3(b)]. The black curves in both graphs are max-hold traces recorded with a hold time of 45 min for a determination of the locking range, while the gray curve denotes the background noise level, which was measured with the photodiode blocked.

For the two rotation angles, the beat frequency was tuned over the displayed range of 400 MHz by varying the crystal temperature and consecutively adapting the crystal lateral position. Note that an rf beat power measurement yields only a single-sided power spectrum. Therefore, for recording each of the two traces shown, the beat frequency tunes in two directions: namely, first with the beat frequency *decreasing* from 200 MHz to zero (while *increasing* the crystal temperature from 178.68 to 178.78 °C) and then with the beat frequency *increasing* from zero to 200 MHz (while *still increasing* the temperature from 178.78 to 178.88 °C). From this observation, the two measurements can be assigned unambiguously to the two opposite sides of the beat amplitude spectrum, and in Fig. 3 the two measurements are plotted as

¹We note that when the cavity length is stabilized to an even number of half wavelengths, there is a set of beat frequencies with spacing 1.7 GHz and that there is a second set of beat frequencies with the same spacing, but located in between the first set for an odd number of half pump wavelengths. By interrupting the Pound-Drever lock, one can switch between the two sets, one of which contains a beat frequency below 425 MHz.

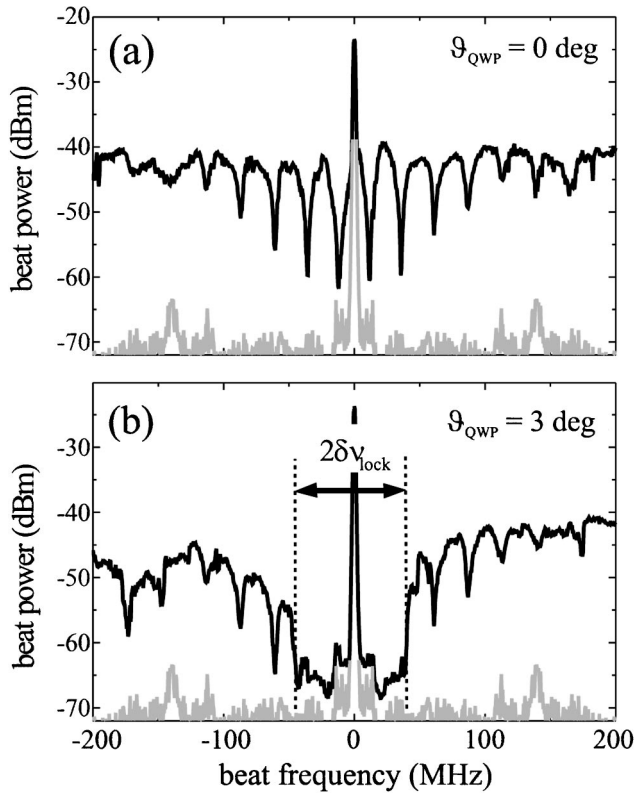


FIG. 3. Measured beat frequency spectra for a quarter-wave plate rotation angle of (a) $\vartheta_{QWP}=0^\circ$ and (b) $\vartheta_{QWP}=3^\circ$. The beat signal power is displayed as a function of the beat frequency by the black curves, and the gray curves are the background noise level, recorded with the photodiode blocked.

two halves of a two-sided beat frequency spectrum, in which the crystal temperature increases from left to right by 0.2°C , while the beat frequency changes from -200 MHz to $+200\text{ MHz}$.

Before we turn to the interpretation of the beat spectra we note that there are also a sharp central peak and a number of dips observable in both Figs. 3(a) and 3(b). The central peak is caused by dc noise pickup as is intrinsic to all rf measurements. The smaller dips appearing with approximately regular spacing of 24 MHz could be linked neither to a decrease of the OPO output power nor to the iterative tuning.

From the upper spectrum in Fig. 3(a) it can be seen that the beat signal was observable with generally 30 dB above the noise level within the entire tuning range of 400 MHz . Particularly, with the QWP rotation angle set to 0° , the OPO could be tuned smoothly through frequency degeneracy, which proves the absence of self-phase-locking. In contrast, with the QWP rotation angle set to 3° [Fig. 3(b)], the beat signal is strongly suppressed to the background noise level within a 80-MHz -wide interval around zero beat frequency. This observation proves that the OPO is self-phase-locked within that interval. The OPO operates stably within this self-phase-locked regime for typically 15 min , before the reappearance of a nonzero beat signal indicates that locking has ceased. The measured interval of beat suppression of 80 MHz corresponds to a full locking range of 80 MHz for the set QWP rotation angle of 3° .

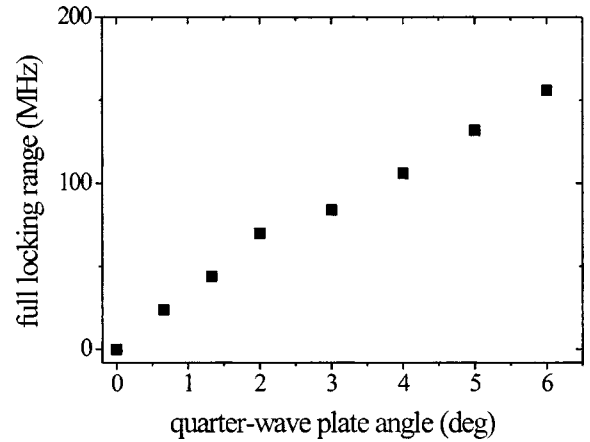


FIG. 4. Measured self-phase locking range of the OPO as a function of the QWP rotation angle.

The described measurement of the locking range has been repeated for various different rotation angles of the QWP—i.e., for different strengths of mutual e- and o-wave injection. Figure 4 shows the measured locking range of a function of the QWP rotation angle. An experimental error of $\pm 1^\circ$ is given by the tiny wave-plate mount that had to be used, due to the limited space inside the OPO cavity. It can be seen that, increasing the QWP rotation angle, the locking range increases steadily. The largest locking range measured is 160 MHz , which is achieved with a QWP angle of 6° .

B. Frequency stability

The frequency and phase stability is a most important characteristic of a frequency divider, as it states the precision one can expect for the frequency-division process of the pump frequency into the subharmonic frequencies. This precision may be limited by residual fluctuations, with which the subharmonic frequencies deviate from the pump frequency exactly divided by 2.

The most direct method to characterize the frequency stability of the divider is to compare the input frequency with the output frequency in a beat measurement. This, however, is not straightforward here, because the pump and subharmonic frequencies are largely different, such that prior to superimposing the input (pump) and output (e.g., the e-wave), the output would have to be frequency doubled. This has two disadvantages. First, doubling the frequency of one of the output waves would yield only very low powers (at the nanowatt level), which would result in a low signal-to-noise ratio. Second, in order to compare only the two desired waves, great efforts would have to be taken to filter out any residual pump light and light of the other subharmonic wave, to avoid a sum frequency mixing of the two subharmonic waves.

We avoided these problems by comparing the two subharmonic waves with each other in a beat measurement. A suitable method for the measurement of a frequency difference is, for example, the measurement of the bandwidth of a beat signal, as has been demonstrated in former experiments, when the beat signal of the subharmonic waves of a self-

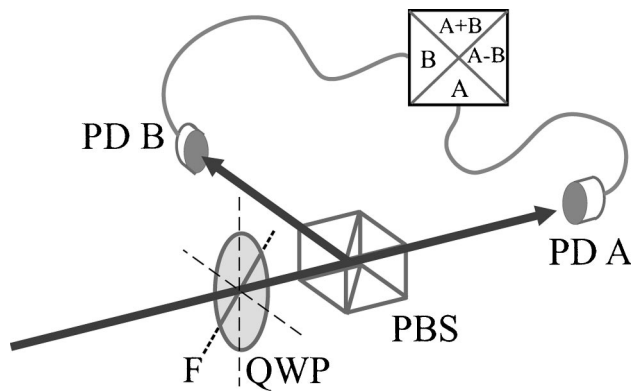


FIG. 5. Setup of the Hänsch-Couillaud-detector. QWP, quarter-wave plate with fast axis F set to 45° ; PBS, polarizing beam splitter; PD A and PD B, photodiodes.

phase-locked divider OPO was shifted out of the dc noise peak at zero beat frequency with an acousto-optic modulator [10,21]. In those experiments, however, the measurement was limited by the 10-Hz resolution of the used rf analyzer. Here, we employ an improved measurement method: namely, a phase-sensitive detector scheme that measures the relative phases of the OPO output waves—i.e., the phase difference $\varphi_e - \varphi_o$. For measurement times considerably longer than the cavity lifetime, the measurable fluctuation of the e-o-difference phase equals 2 times the deviation of either one of the subharmonic-waves phases from the target phase $\frac{1}{2}\varphi_p(t)$.

The phase-sensitive detector scheme we employ to measure the relative phase stability of the OPO output waves was introduced by Hänsch and Couillaud in 1980 [22] for the purpose of electronic cavity stabilization. The setup of the Hänsch-Couillaud detector (HC detector) is shown schematically in Fig. 5. The two OPO subharmonic waves pass a quarter-wave plate, which is set such that its fast axis forms an angle of 45° with either one of the OPO waves. After passing the QWP, the beam is sent to a polarizing beam splitter, followed by two fast germanium photodiodes with a cutoff frequency of 500 MHz. The two photodiode currents are electronically processed to yield their sum and difference.

This way, the difference signal varies as a cosine function of the phase difference ($\varphi_e - \varphi_o$). The amplitudes of both signals are proportional to the geometrical average of the e- and o-wave intensities. Therefore, if we divide the difference by the sum signal, this yields an output that is independent of the output power of the OPO. Note that it is not possible to distinguish the two different phase steady states a divide-by-2 OPO can assume [14], as the phase difference ($\varphi_e - \varphi_o$) determined by this detector is equal for both states. Note also that the HC difference signal can be related unambiguously to a phase difference only modulo π . For the observation of the drift of the phase difference of the divider's subharmonic waves, however, this is fully sufficient, as the phase difference ($\varphi_e - \varphi_o$) remains within an interval of π during self-phase-locked operation of the OPO.

Figure 6(a) shows an example of the HC difference signal measured as a function of time, while Figs. 6(b) and 6(c)

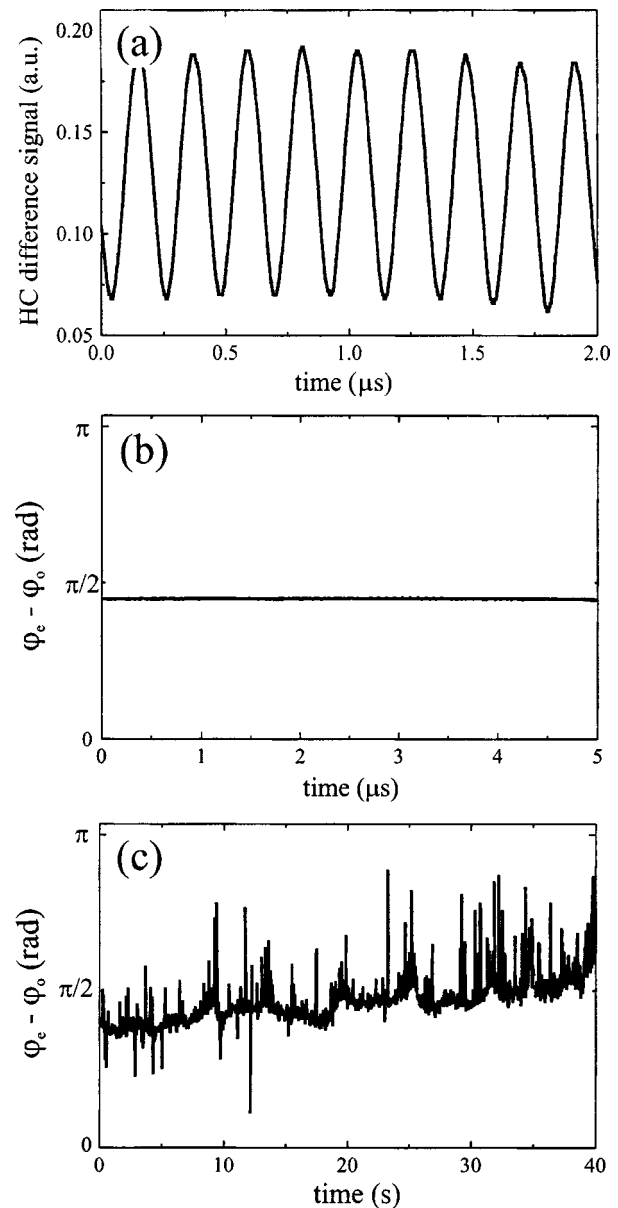


FIG. 6. (a) Measured signals of the HC detector as a function of time while the OPO is not locked (without QWP), (b) and (c) phase difference retrieved from the HC signal while the OPO is phase locked (with the QWP set to 3°).

show two examples of the retrieved phase difference (i.e., the difference signal divided by the sum signal) versus time. In the first example of Fig. 6(a), the quarter-wave plate is not yet inserted in the OPO cavity (and thus the OPO is not phase locked). It can be seen that the frequency difference signal varies much slower than the cutoff frequency of the HC detector photodiodes, as was also confirmed by measuring the beat signal with the rf analyzer. The regular oscillation of the cosine-shaped HC signal is an indication of an approximately constant frequency difference between the e- and o-waves. From the measurement in Fig. 6(a) we obtain a period of the cosine function of $0.2 \mu\text{s}$, which corresponds to a beat frequency of $\nu_{beat} = |\nu_e - \nu_o| = 5 \text{ MHz}$.

In contrast, Figs. 6(b) and 6(c) show two examples of the phase difference $\varphi_e - \varphi_o$ obtained over different measurement

intervals when the OPO was phase locked. During these measurements, the intracavity quarter-wave plate was set to 3° , and phase locking was verified by observing a 27-MHz beat frequency after frequency shifting one of the output beams using an acousto-optic modulator operating at this frequency of 27 MHz. The graphs show two examples for a shorter measurement time interval of $5 \mu\text{s}$ [Fig. 6(b)] and for a much longer measurement time interval of 40 s [Fig. 6(c)]. From the example shown in Fig. 6(b), one can see that the phase difference is essentially constant over the measurement time of $5 \mu\text{s}$. During this time, the phase difference stays within an interval of less than 0.02 rad. This phase difference stabilization [in contrast to Fig. 6(a)] indicates that the OPO is self-phase-locked and that the pump frequency is *phase coherently* divided by 2 into the subharmonic frequency.

Over the long measurement period shown in Fig. 6(c), a slow drift of the phase difference can be seen with also some faster phase fluctuations. During the measurement interval of 40 s, the phase difference increases by a total of about 0.71 rad. This corresponds to an average temporal rate of change of the phase difference ($\varphi_e - \varphi_o$) of as low as 0.018 rad/s or 2.8 mHz. Dividing this value by the subharmonic wave frequency, we obtain a residual frequency instability of the e-wave with respect to the o-wave of 1.5×10^{-17} . This corresponds to a residual phase fluctuation of the e-wave (or the o-wave) with respect to a pump wave exactly divided by 2 of 1.4 mHz and to a residual fractional frequency instability of the division process of about 8×10^{-18} in 40 s.

C. Phase difference and power ratio within the locking range

With our present setup we have shown that phase-coherent division by 2 can be realized with a self-phase-locked OPO over tens of seconds. This time span is probably limited by a residual (temporal) drift of the OPO setup parameters, which ultimately causes the OPO to leave the locking range. It has been shown theoretically [13,14] that locking ceases if the ratio of the cavity detunings—i.e., the detunings of the closest cold cavity modes of the e- and o-waves from the pump frequency exactly divided by 2—drift out of a certain interval: $C_1 < \Delta_e/\Delta_o < C_2$, where Δ_e and Δ_o are the cavity detunings for the e- and o-waves, respectively, and where C_1 and C_2 are constants given by construction parameters of the OPO cavity.

For an application of the OPO divider—e.g., in a frequency metrology experiment—an operation time span of tens of seconds is not sufficient, because a reliable division would be required over much longer time intervals, such as hours and days. However, as the drift is rather slow, with typically tens of seconds compared to the response time of the self-phase-locking (i.e., the inverse locking range of about 10 ns), a slow controller (e.g., computer based) would be sufficient to counteract this residual drift, preventing the OPO from leaving the locking range.

Such a control loop would require a different type of error signal than the actively phase-locked frequency dividers, where the error signal is usually obtained via a beat measure-

ment [6,8]. In our case of all-optical phase locking there is no beat signal available, which could serve as the error signal. Thus it is required to identify a suitable error signal, which contains information about the divider's slow drift within the locking range.

In the following, we show that the power ratio of the subharmonic output waves can be used to monitor the drift of the self-phase-locked OPO within its optical locking range. For this we recall that in self-phase-locked operation, the OPO subharmonic phases attain steady-state values which are functions of the cavity detunings Δ_e and Δ_o . The phase difference is given by [see, e.g., Eq. (5) in Ref. [12], Eq. (2.14) in Ref. [13], or Eq. (10) in Ref. [14]]:

$$\varphi_e - \varphi_o = \theta \pm \arccos \left[\frac{1}{4\gamma_0} \left(\kappa_e \sqrt{\frac{\Delta_o}{\Delta_e}} - \kappa_o \sqrt{\frac{\Delta_e}{\Delta_o}} \right) \right]. \quad (1)$$

Here, κ_e and κ_o are the cavity decay rates for the e- and o-waves, and the parameter γ_0 is a measure for the coupling strength between the two waves and increases with the experimentally adjustable angle of the quarter-wave plate's fast axis. θ is a phase shift the subharmonic waves acquire while traveling through the QWP and, as it is just a constant in Eq. (1), should show in an experiment only as an offset. For the given experimental parameters and a QWP rotation angle of 3° , we have derived the following numbers, which will be used for a comparison of experiment and theory: $\kappa_e = 114$ MHz, $\kappa_o = 117$ MHz, and $\gamma_0 = 12.1$ MHz.

Furthermore, the ratio of the e- and o-wave intracavity photon numbers N_e and N_o , which are proportional to the output powers P_e and P_o , is a function of the cavity detunings Δ_e and Δ_o [14]:

$$\frac{\Delta_o}{\Delta_e} = \frac{N_e}{N_o} = \frac{P_e}{P_o}. \quad (2)$$

Having both the phase difference and the power ratio expressed as functions of the cavity detunings, a measurement of the output power ratio should reveal the phase difference and should also enable one to monitor the OPO's drift within its optical locking range. To measure the expected dependence of the relative phase and the power ratio we change the cavity detunings by scanning the lateral position of the wedged crystal using a piezoactuator. To enable a simultaneous measurement, a 50% portion of the OPO output is sent to two germanium photodiodes behind a polarizing beam splitter for recording the power ratio. The remaining part of the OPO output is used for a measurement of the OPO's phase difference with the HC detector, as was described before in Sec. III B.

While scanning the crystal position with a triangular function, two photodiode signals for measurement of the e-wave and o-wave power, and the difference and the sum signal of the HC detector were recorded together with the piezovoltage using a data-acquisition card. These five signals were recorded with 2000 data points per second each, while the OPO was self-phase-locked, with the QWP set to a rotation angle of 3° .

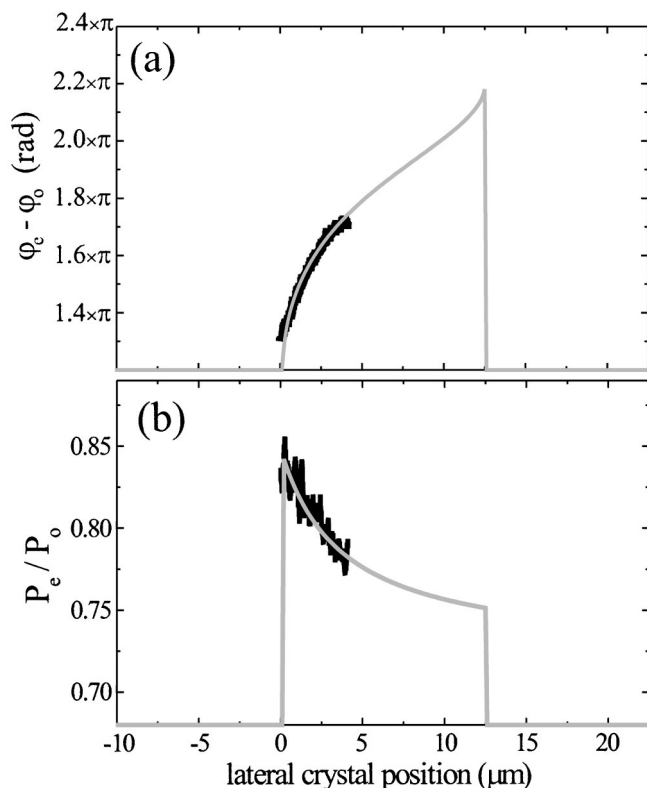


FIG. 7. (a) Phase difference and (b) power ratio as a function of the lateral crystal position. Black trace: measured values. Gray trace: theoretically calculated values.

In Fig. 7(a), the measured phase difference $\varphi_e - \varphi_o$ is displayed as a function of the lateral crystal position by the black trace. The gray trace is the theoretically expected phase difference fit to the experimental data, which has been calculated using Eq. (1). The free parameters used in the fit are a constant crystal temperature offset, a constant offset for the phase difference, and a constant offset for the lateral crystal position. As can be seen, the experimentally observed phase difference is in full agreement with the theoretical prediction. In Fig. 7(b), the black trace shows the power ratio, which was measured simultaneously with the phase difference, as a function of the crystal position. The gray trace is the theoretically expected power ratio [from Eq. (2)], fitted to the experimental data for the same crystal temperature and using the same offset for the crystal position as in Fig. 7(a). Here, the only fit parameter is a constant factor for the power ratio, which takes into account, e.g., the different losses and detection efficiencies for the two power signals. Again, there is a good agreement between the measured power ratio and the theoretical prediction.

The presented measurements and their agreement with theory show that it is possible to monitor the e- and o-wave cavity mode detunings *without* the need of a beat measure-

ment. At the same time, it has been demonstrated that these detunings can be controlled via external parameters, in our case the translation of the crystal. Combined, this forms a valuable tool which should enable to stabilize the self-phase-locked operation of the divider against thermal drifts of the cavity length. This could be realized, e.g., by employing a slow (possibly computer-based) servoloop, which receives its error signal from a measurement of the power ratio and which would control the crystal position.

IV. SUMMARY

We have presented the experimental realization of wavelength-flexible frequency division by 2 based on a self-phase-locked cw OPO. Self-phase-locked frequency division by 2 was proven by measuring the suppression of the beat of the two OPO output waves in a range around zero beat frequency. Typically, the divider operates within the stable self-phase-locked state for 15 min before it falls out of self-locking due to a thermally induced drift of the cavity length. The locking range has been measured to increase in proportion with the QWP rotation angle, and the largest locking range achieved at a QWP angle of 6° was 160 MHz.

The frequency stability of a frequency divider has been quantitatively determined by a measurement of the phase difference of the two subharmonic waves. This measurement yielded a residual thermal drift of the relative phase of the two subharmonic waves of 0.7 rad in 40 s. This corresponds to an extremely low residual fractional frequency instability of 8×10^{-18} of the divide-by-2 OPO.

For the first time, the subharmonic phase difference and the output power ratio of the self-phase-locked divider OPO have been measured as a function of the cavity detunings, which were piezocontrolled via a transverse translation of the nonlinear crystal. The experimental data are in excellent agreement with theory. In particular, due to its experimental ease, it seems of interest to measure the output power ratio of the e- and o-waves as an error signal for a slow electronic servoloop. Such a loop could act on the transverse displacement of the crystal, with the goal of maintaining the OPO within its self-locking range for extended times, from which a significant improvement of the long-term stability of the divider can be expected.

ACKNOWLEDGMENTS

The authors acknowledge financial support by the Dutch Stichting voor Fundamenteel Onderzoek der Materie (FOM) and by the Deutsche Forschungsgemeinschaft (DFG). We thank Professor Dr. R. Wallenstein for his generous loan of equipment. We gratefully thank Dr. H. L. Offerhaus for stimulating discussions on the working principle of frequency dividers.

- [1] A. Heidmann, R. J. Horowicz, E. Giacobino, C. Fabre, and G. Camy, *Phys. Rev. Lett.* **59**, 2555 (1987).
- [2] K. W. Leong, N. C. Wong, and J. H. Shapiro, *Opt. Lett.* **15**, 1058 (1990).
- [3] N. Ph. Georgiades, E. S. Polzik, K. Edamatsu, H. J. Kimble, and A. S. Parkins, *Phys. Rev. Lett.* **75**, 3426 (1995).
- [4] N. C. Wong, *Opt. Lett.* **15**, 1129 (1990).
- [5] R. Graham and H. Haken, *Z. Phys.* **210**, 276 (1968).
- [6] D. Lee and N. C. Wong, *Opt. Lett.* **17**, 13 (1992).
- [7] S. Slyusarev, T. Ikegami, and S. Ohshima, *Opt. Lett.* **24**, 1856 (1999).
- [8] A. Douillet, J.-J. Zondy, G. Santarelli, A. Makdissi, and A. Clairon, *IEEE Trans. Instrum. Meas.* **50**, 548 (2001).
- [9] A. E. Siegman, *Laser Injection Locking* (University Science Books, Mill Valley, CA, 1986), Chap. 29, pp. 1130–1170.
- [10] D.-H. Lee, M. E. Klein, J.-P. Meyn, R. Wallenstein, P. Groß, and K.-J. Boller, *Phys. Rev. A* **67**, 013808 (2003).
- [11] C. D. Nabors, S. T. Yang, T. Day, and R. L. Byer, *J. Opt. Soc. Am. B* **7**, 815 (1990).
- [12] E. J. Mason and N. C. Wong, *Opt. Lett.* **23**, 1733 (1998).
- [13] C. Fabre, E. J. Mason, and N. C. Wong, *Opt. Commun.* **170**, 299 (1999).
- [14] P. Gross and K.-J. Boller, *Phys. Rev. A* **71**, 033801 (2005).
- [15] M. Scheidt, B. Beier, K.-J. Boller, and R. Wallenstein, *Opt. Lett.* **22**, 1287 (1997).
- [16] K. Liu and M. G. Littman, *Opt. Lett.* **6**, 117 (1981).
- [17] R. W. P. Drever, J. L. Hall, F. V. Kowalski, J. Hough, G. M. Ford, A. J. Munley, and H. Ward, *Appl. Phys. B: Photophys. Laser Chem.* **31**, 97 (1983).
- [18] D.-H. Lee *et al.*, *Proc. SPIE* **3928**, 25 (2000).
- [19] G. J. Edwards and M. Lawrence, *Opt. Quantum Electron.* **16**, 373 (1984).
- [20] D.-H. Lee, M. E. Klein, J.-P. Meyn, P. Groß, R. Wallenstein, and K.-J. Boller, *Opt. Express* **5**, 114 (1999).
- [21] P. Groß, K.-J. Boller, M. E. Klein, and D.-H. Lee, *Conference on Lasers and Electro-optics: Postdeadline Papers Book* (Optical Society of America, Washington, DC, 2003), postdeadline paper no. CPDB1.
- [22] T. W. Hänsch and B. Couillaud, *Opt. Commun.* **35**, 441 (1980).